Available online at www.sciencedirect.com
SCIENCE DIRECT®
Journal of Computational Physics 188 (2003) 194–208
JOURNAL OF COMPUTATIONAL PHYSICS
www.elsevier.com/locate/jcp

# Strongly consistent marching schemes for the wave equation

Jing-Rebecca Li *,[1], Leslie Greengard [2]

*Courant Institute of Mathematical Sciences, New York University, 251 Mercer Street, New York, NY 10012-1110, USA*

Received 3 March 2002; received in revised form 28 January 2003; accepted 4 March 2003

**Abstract**

In this paper, we consider a class of explicit marching schemes first proposed in [1] for solving the wave equation in complex geometry using an embedded Cartesian grid. These schemes rely on an integral evolution formula for which the numerical domain of dependence adjusts automatically to contain the true domain of dependence. Here, we refine and analyze a subclass of such schemes, which satisfy a condition we refer to as strong $u$-consistency. This requires that the evolution scheme be exact for a single-valued approximation to the solution at the previous time steps. We provide evidence that many of these strongly $u$-consistent schemes are stable and converge at very high order even in the presence of small cells in the grid, while taking time steps dictated by the uniform grid spacing.


*Keywords:* Small cell; Stability; Wave equation

## 1. Introduction

The solution of the wave equation in complex geometry has important applications in electromagnetics, acoustics and a variety of other application areas. In some cases, frequency domain analysis is sufficient, but in others, the solution is better studied in the time domain. Examples include the analysis of wide band signals, transient behavior, and the treatment of material inhomogeneities and nonlinearities.

In solving the wave equation in complex geometry, Cartesian grids with embedded boundaries have a number of advantages over body fitted grids; they allow for more efficient implementation as well as automatic grid generation. In complicated domains, however, it is inevitable that there will be small cells where the Cartesian grid intersects the irregular boundary. Explicit finite difference schemes are then restricted in the size of the time step they can take due to the CFL condition. For typical schemes with a fixed

* Corresponding author.
*E-mail addresses:* jingli@cims.nyu.edu (J.-R. Li), greengard@cims.nyu.edu (L. Greengard).
[1] The work of this author was supported by the US Department of Energy under Grant DE-FGO2-00ER25053 and by the National Science Foundation under Grant DMS-9983190.
[2] The work of this author was supported in part by the US Department of Energy under Grant DE-FG02-00ER25053 and HRL under Contract MDA972-01-C-0006.

0021-9991/03/$ - see front matter 
doi:10.1016/S0021-9991(03)00163-3

stencil, the size of the time step is usually dependent on the size of the smallest cell in the spatial discretization [7,8]. We would like to overcome this restriction and allow time steps on the order of the size of the uniform cells in the grid even when small cells are present near the boundary.

A necessary but not sufficient condition to ensure stability in the presence of small cells is to enlarge the numerical domain of dependence to include the true domain of dependence of the PDE near the small cells. There are numerous approaches to this 'small cell' problem for conservation laws, mostly in two dimensions. They include cell merging (see, e.g. [3,6]), large time step generalizations of Godunov's method [5], and the rotated grid $h$-box method [2]. Cell merging approaches remove small cells near the boundary and tend to result in a loss of accuracy there. The other approaches keep the small cells in the grid and enlarge the numerical domain of dependence near the small cells in some way. These approaches, however, were developed for nonlinear conservation laws, where shock resolution is an essential feature and low order accuracy is an acceptable option. For large-scale wave propagation problems, high accuracy is much more critical to avoid numerical dispersion errors.

In [1], a class of explicit marching schemes was proposed to solve the wave equation which appeared to be remarkably insensitive to the presence of small cells in the computational grid. This class of schemes was derived from a new, exact, three time level evolution formula, which automatically incorporates the true domain of dependence of the wave equation into the numerical domain of dependence of the scheme. While a promising approach, we found that not all schemes of this type were stable, suggesting that a more detailed analysis was required.

In this paper, we modify the evolution formula of [1] to account for discretization effects, particularly the discontinuities found in piecewise polynomial approximations to the solution. We also show how to apply the evolution formula to the case where there are multiple wave speeds in the problem. The main contribution here is a paradigm for generating a large set of stable, high order, explicit marching schemes for the wave equation which are robust in the presence of small cells in the computational grid. Contained in this paradigm is a specification for generating the evolution stencil at all grid points, regardless of whether the grid points are near small cells. We are not aware of any comparable procedure for generating stable, explicit, and high order marching schemes based on finite difference or finite element discretizations.

This paper is organized as follows. Section 2 describes the evolution formula given in [1] and Section 3 introduces the idea of *strong consistency* of an evolution scheme. Sections 4 and 5 present specific classes of such schemes which we refer to as strongly consistent and strongly $u$-consistent, respectively. Section 6 extends our approach to problems with abrupt changes in material properties, where multiple wave speeds are present. Section 7 gives numerical results concerning the stability and accuracy and Section 8 contains our conclusions.

It is important to note that the present paper is largely experimental. The schemes we believe to be stable have been studied by matrix analysis for a broad range of grids; a direct proof has yet to be found.

## 2. Exact integral evolution formula

It was shown in [1] that if $u(x,t)$ is a solution to the homogeneous wave equation

$$u_{tt} = \nabla^2 u \tag{1}$$

in $\mathbb{R}^d$, then there exists a kernel $G_d(|x-y|,\tau)$ such that

$$u(x,t+\tau) = 2u(x,t) - u(x,t-\tau) + \int_{B_\tau(x)} G_d(|x-y|,\tau)\nabla^2 u(y,t)\,\mathrm{d}y, \tag{2}$$

where $B_\tau(x) = \{y, |y-x| \leqslant \tau\}$ denotes the closed ball in $\mathbb{R}^d$ of radius $\tau$ centered at $x$. Moreover,

$$G_1(r,\tau) = \tau - r,$$

$$G_2(r,\tau) = \frac{\ln(\tau + \sqrt{\tau^2 - r^2}) - \ln r}{\pi},$$

$$G_3(r,\tau) = \frac{1}{2\pi r}.$$

**Remark 2.1.** If $u(x,t)$ is a periodic function on some box in $\mathbb{R}^d$, the formula (2) still holds, with the Laplacian term $\nabla^2 u$ interpreted in the periodic sense.

Suppose now that we want to solve the wave equation (1) in a finite domain $D$ subject to Dirichlet conditions $u(x,t) = g(x,t)$ on the boundary $\partial D$. We can modify the formula (2) by restricting the region of integration. We define $\tilde{u}(x,t+\tau)$ by

$$\tilde{u}(x,t+\tau) \equiv 2u(x,t) - u(x,t-\tau) + \int_{B_\tau(x)\cap\mathscr{D}} G_d(|x-y|,\tau)\nabla^2 u(y,t)\,\mathrm{d}y. \tag{3}$$

It is easy to verify that $\tilde{u}$ satisfies the wave equation for $\tau > 0$ and that

$$\Psi(x,t+\tau) \equiv u(x,t+\tau) - \tilde{u}(x,t+\tau), \quad x \in D$$

takes on zero initial data. At the boundary, however, we must have

$$\Psi(x,t+\tau) = g(x,t+\tau) - \tilde{u}(x,t+\tau), \quad x \in \partial D. \tag{4}$$

The wave equation for $\Psi$ can be solved using hyperbolic potential theory [4]. For short times $\tau$, this involves a *local boundary integral* for which the cost is negligible. In one space dimension, the solution is available analytically; assuming that $x > a$, where $a$ is the left boundary point, an elementary calculation [4] shows that

$$\Psi(x,t+\tau) = \begin{cases} 0 & \text{if } x - a \geqslant \tau, \\ g(a,t+\tau-x+a) - \tilde{u}(a,t+\tau-x+a) & \text{if } x - a \leqslant \tau. \end{cases} \tag{5}$$

(On the interval $[a,b]$, a similar formula applies near the right boundary point $x = b$.)

**Definition 2.1.** We refer to the function $\Psi(x,t+\tau)$ as the boundary correction term.

Our numerical approach to solving the wave equation (1) is straightforward. For problems in free-space or with periodic boundary conditions, we discretize (2) for a time step $\tau = \Delta t$ and use the result as a three time level scheme. In the presence of boundaries, we discretize (3), add the boundary correction term $\Psi(x,t+\tau)$, and use that result to march forward in time.

**Remark 2.2.** For the sake of simplicity, we assume $u(x,0)$ and $u(x,\Delta t)$ are given, ignoring "startup issues" for the three level scheme.

In the present paper, we will limit our attention to periodic and Dirichlet boundary conditions in one space dimension on a interval $[a,b]$. For this, we introduce a simple computational mesh $x_1 = a, x_2, \ldots, x_{M-1}, x_M = b$. For the sake of simplicity, the mesh is equispaced with the possible exception of the first and last subintervals; i.e., $x_3 - x_2 = x_4 - x_3 = \cdots = x_{M-1} - x_{M-2}$, but $x_2 - x_1$ and $x_M - x_{M-1}$ are

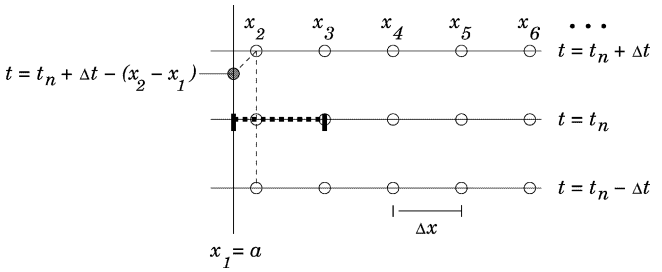


Fig. 1. An irregular computational grid for Dirichlet problems. While most points are equispaced, the first grid point $x_2$ is near the physical boundary. For that point, the thick horizontal dashed line indicates the range of integration in (3). (Only the grid near the left boundary is shown.)

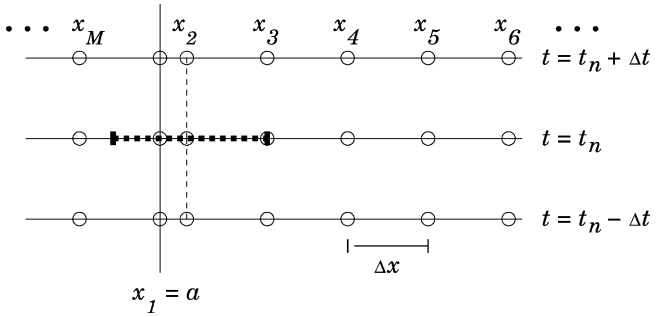


Fig. 2. An irregular computational grid for periodic problems. While most points are equispaced, the first grid point is arbitrarily close to the periodic boundary. For that point, the thick horizontal dashed line indicates the range of integration in (3). (Only the grid near the left boundary is shown and $x_{M+1}$ is identified with $x_1$.)

arbitrary (see Figs. 1 and 2). This is a reasonable model for higher dimensional problems, where a uniform Cartesian mesh is superimposed on a complex region, creating small cells in the vicinity of the boundary.

**Definition 2.2.** We will denote by $U_i^n$ the value of the approximate solution at the grid point $x_i$ at time $t_n = n\Delta t$.

In [1], the following approach was proposed.

**Algorithm**

1. From the current data $U_i^n$, compute a discrete approximation of the Laplacian $\nabla^2 U_i^n$.
2. From the discrete Laplacian data $\nabla^2 U_i^n$, compute a piecewise polynomial interpolant $\nabla^2 U(x, t_n)$.
3. Replace $\nabla^2 u(y, t)$ in the formula (3) with $\nabla^2 U(y, t)$.
4. Integrate the resulting formula analytically for a time step $\tau = \Delta t$. This is straightforward for piecewise polynomial data:

$$U_i^{n+1} := 2U_i^n - U_i^{n-1} + \int_{B_\tau(x)\cap\mathscr{D}} G_d(|x-y|,\tau)\nabla^2 U(y,t_n)\,\mathrm{d}y.$$

5. For Dirichlet problems, add the boundary correction using (5).

$$U_i^{n+1} := U_i^{n+1} + \Psi(x_i, t_{n+1}).$$

6. Repeat.

Numerical experiments suggested that this approach can lead to fourth-order accurate schemes which are robust and stable even in the presence of small cells. However, higher order stable schemes were difficult to obtain. This led us to investigate evolution schemes for which a polynomial approximation is made to $U_i^n$ directly, rather than to the discrete Laplacian $\nabla^2 U_i^n$. This appears to allow for higher order accuracy while maintaining stability.

## 3. Strongly consistent evolution schemes

Before proceeding, it is worth reconsidering finite difference schemes for the wave equation from a somewhat non-standard viewpoint. Classical analysis is based on the notions of stability and consistency, and does not pay attention to the following simple question: is there an underlying single-valued function $u$ for which the marching scheme can be interpreted as an evolution process? It turns out the answer is no—the reader will easily verify that a moving finite difference stencil corresponds to a multiple-valued interpretation of both $\nabla^2 u(x,t_n)$ and $u(x,t_n)$. This leads us to introduce the following definitions.

**Definition 3.1.** A numerical scheme based on the integral evolution formula (3) is *strongly consistent* if it incorporates a function $\nabla^2 u(x,t_n)$ which is single valued in the entire domain.

**Definition 3.2.** A numerical scheme based on the integral evolution formula (3) is *strongly u-consistent* if it incorporates functions $u(x,t_n)$ and $u(x,t_{n-1})$, both of which are single valued in the entire domain.

**Remark 3.1.** The approach in [1] described above yields strongly consistent, but not strongly $u$-consistent schemes.

We will use $U(x,t_n)$ to denote a single-valued function, defined in all of $\mathscr{D}$, which approximates the discrete data $U_i^n$, $i=1,\ldots,M-1$. In each cell (subinterval) of the Cartesian grid, we represent $U(x,t_n)$ as a polynomial. This polynomial is obtained by fitting, in a least squares sense, a subset of the current data points $U_i^n$ using grid points in or near that cell. More precisely, let $\mathscr{D}=[a,b]$ and let the spatial grid be $\{a=x_1,\ldots,x_M=b\}$. A cell is an interval $[x_i,x_{i+1}], i=1,\ldots,M-1$, and we denote the polynomial approximation on the interval $[x_i,x_{i+1}]$ by $U^i(x,t_n)$. Expressions like $U_x^i(x_i,t_n)$, $U_{xx}^i(x_i,t_n)$, $U_x^i(x_{i+1},t_n)$, $U_{xx}^i(x_{i+1},t_n)$, which will appear later, are used to denote the (one-sided) first and second derivatives of $U^i(x,t_n)$ at the interval boundaries $x=x_i,x_{i+1}$.

We now define a scheme $S_m^p$ according to the order $p$ of the piecewise polynomial approximation in each cell and the number of points $p+1+m$ used to obtain a least squares fit. The polynomial $U^i(x,t_n)$ is obtained by fitting the values of $U_{i-i_l}^n,\ldots,U_i^n,U_{i+1}^n,\ldots,U_{i+1+i_r}^n$, where $i_l+2+i_r=p+1+m$. The number of points to the left of the cell is $i_l=\max(\lfloor(p+1+m-2)/2\rfloor,i)$. The number of points to the right of the cell is $i_r=p+1+m-2-i_l$ if $i_r\leqslant M$; otherwise, we set $i_r=M-i-1$. In short, the points used to obtain a least squares fit are as symmetric as possible around the interval $[x_i,x_{i+1}]$ without leaving the domain. If $p+1+m$ is even, the stencil is symmetric away from the boundary. Otherwise, the stencil is non-symmetric. We say that a scheme is *interpolatory* if $m=0$, because then $U(x,t_n)$ interpolates all data points exactly. If $m\geqslant 1$, we refer to the scheme as a *least squares scheme*.

When $U(x,t_n)$ is obtained by a least squares scheme, it is discontinuous, and we define the value at the grid points themselves as the average of the one-sided limits. In this case, $U_x(x,t_n)$ is a generalized function which we consider in more detail in Section 5.

## 4. Strong consistency

Given the function approximation $U(x,t_n)$ in the preceding section, we can ignore discontinuities at interval boundaries and define $\nabla^2 U(x,t_n)$ as the piecewise smooth function defined by

$$\nabla^2 U_{PS}(x,t_n) = U^i_{xx}(x,t_n) \quad \text{for } x \in (x_i, x_{i+1}). \tag{6}$$

This function is obviously single valued in the entire domain $[a,b]$. A scheme $S^p_m$ using (6) to compute the integral in (3), with any choice of $\Delta t$ and spatial discretization, is strongly consistent according to Definition 3.1. Recall that in each cell, the convolution integral in (3) can be computed exactly for polynomials. Thus, the accuracy of the evolution scheme depends only on the order $p$ of the piecewise polynomial approximation.

Such a scheme is not strongly $u$-consistent because the function $U(x,t_n)$ and its derivatives may have discontinuities across the boundaries between cells which are not taken into account. In other words, the expression in (6) is not the actual Laplacian of $U(x,t_n)$ in the sense of generalized functions.

## 5. Strong *u*-consistency

In this section, we modify the formula in (3) to account for the piecewise smooth nature of $U(x,t_n)$ in order to satisfy the more stringent requirement of strong $u$-consistency.

The region of integration for the convolution integral in (3), namely $\overline{B}_{\Delta t} \cap \mathscr{D}$, encompasses the boundaries of several cells. On these boundaries, $U(x,t_n)$ may have jump discontinuities, which lead to Dirac $\delta$-function singularities in its first derivatives and $\delta'$ singularities in its Laplacian. Similarly, the first derivatives of $U(x,t_n)$ will have jump discontinuities which lead to additional $\delta$ singularities in the Laplacian.

One could, of course, avoid discontinuities by enforcing the condition that $U(x,t_n) \in C^2(\mathscr{D})$. Since it is impractical to enforce such a condition in two and three dimensions, we make no effort in this paper to do so. The present one-dimensional analysis then serves as a more realistic model. The analytical derivative of $U(x,t_n)$ contains jumps at interior grid points of the form

$$J^{x_i}_{U(x,t_n)}\delta(x-x_i), \quad \text{where } J^{x_i}_{U(x,t_n)} = U^i_x(x_i,t_n) - U^{i-1}_x(x_i,t_n). \tag{7}$$

The analytical second derivative of $U(x,t_n)$, i.e., $\nabla^2 U(x,t_n)$ contains discontinuities of the form

$$J^{x_i}_{U(x,t_n)}\delta'(x-x_i) + J^{x_i}_{U_x(x,t_n)}\delta(x-x_i), \tag{8}$$

where $J^{x_i}_{U_x(x,t_n)} = U^i_x(x_i,t_n) - U^{i-1}_x(x_i,t_n)$ is the magnitude of the discontinuity of the piecewise polynomial part of $U_x(x,t_n)$ at $x_i$.

In summary, we define

$$\nabla^2 U(x,t_n) = \nabla^2 U_{PS}(x,t_n) + \sum_{i=1}^{M-1} J^{x_i}_{U(x,t_n)}\delta'(x-x_i) + J^{x_i}_{U_x(x,t_n)}\delta(x-x_i). \tag{9}$$

It remains only to compute the effect of the singular terms on the integral in (3). If we let $y_0 = \max(a, x_i - \Delta t)$ and $y_f = \min(b, x_i + \Delta t)$, then the contribution from a $\delta$-function discontinuity is

$$\int_{y_0}^{y_f} (\Delta t - |x_i - y|) J^z_{U_x(x,t_n)}\delta(y-z)\,\mathrm{d}y = \begin{cases} 0 & \text{if } z \notin [y_0, y_f], \\ (\Delta t - |x_i - z|) J^z_{U_x(x,t_n)} & \text{otherwise.} \end{cases} \tag{10}$$

The magnitude of this quantity is $O(\Delta t J_{U_x(x,t_n)})$. Note that this is extremely small since $J_{U_x(x,t_n)}$ is at most of the order $(\Delta x)^p$, where $p$ is the degree of the piecewise polynomial $U(x,t_n)$.

Similarly, the contribution to (3) due to a discontinuity of $U(x,t_n)$ at the point $z$ is

$$\begin{aligned}
&\int_{y_0}^{y_f} (\Delta t - |x_i - y|) J^z_{U(x,t_n)} \delta'(y-z)\,\mathrm{d}y \\
&\quad = (\Delta t - |x_i - y|) J^z_{U(x,t_n)} \delta(y-z)\Big|_{y_0}^{y_f} - \int_{y_0}^{y_f} (\Delta t - |x_i - y|)_y J^z_{U(x,t_n)} \delta(y-z)\,\mathrm{d}y \\
&\quad \begin{cases} = 0 & \text{if } z \notin [y_0, y_f], \\ = J^z_{U(x,t_n)} \times \begin{cases} -0.5 & \text{if } z = x_i - \Delta t, \\ -1 & \text{if } x_i - \Delta t < z < x_i, \\ 0 & \text{if } z = 0, \\ 1 & \text{if } x_i < z < x_i + \Delta t, \\ 0.5 & \text{if } z = x_i + \Delta t, \end{cases} & \text{if } z \in [y_0, y_f]. \end{cases}
\end{aligned} \tag{11}$$

The magnitude of this quantity is at most of the order $O(J_{U(x,t_n)}) = O((\Delta x)^{p+1})$. If $\Delta t = O(\Delta x)$, this quantity has the same order of magnitude as the integral in (10). These are extremely small corrections, but they have a remarkable impact on stability.

## 6. Multiple wave speeds

The integral evolution formula can be applied to problems with multiple wave speeds. We illustrate with the following example in which there are two wave speeds present, $c_1$ and $c_2$:

$$u_{tt}(x,t) = c_1^2 u_{xx}(x,t), \quad x < 0, \tag{12}$$

$$u_{tt}(x,t) = c_2^2 u_{xx}(x,t), \quad x > 0. \tag{13}$$

We assume that the solution is continuous and differentiable at the interface $x = 0$:

$$\lim_{x\to 0^-} u(x,t) = \lim_{x\to 0^+} u(x,t) := u(0,t), \tag{14}$$

$$\lim_{x\to 0^-} u_x(x,t) = \lim_{x\to 0^+} u_x(x,t) := u_x(0,t). \tag{15}$$

We now derive an exact formula analogous to (2) for the solution of 12–15. Suppose a solution $u(x,t)$ satisfying 12–15 is known for $t \leqslant 0$. We begin by defining two intermediate solutions. First, we define a solution of equation (12) for the left half line,

$$u_1(x,t+\tau) := \begin{cases} u(x,t+\tau), & x \leqslant 0,\ \tau \leqslant 0, \\ 2u(x,t) - u(x,t-\tau) & \\ \quad + \int_{x-c_1\tau}^{\min(0,x+c_1\tau)} (c_1\tau - |y-x|)\nabla^2 u(y,t)\,\mathrm{d}y, & x \leqslant 0,\ \tau > 0. \end{cases} \tag{16}$$

Similarly, we define a solution of (13) on the right half line,

$$u_2(x,t+\tau) := \begin{cases} u(x,t+\tau), & x \geqslant 0,\ \tau \leqslant 0, \\ 2u(x,t) - u(x,t-\tau) & \\ \quad + \int_{\max(0,x-c_2\tau)}^{x+c_2\tau} (c_2\tau - |y-x|)\nabla^2 u(y,t)\,\mathrm{d}y, & x \geqslant 0,\ \tau > 0. \end{cases} \tag{17}$$

We could simply concatenate the two solutions by defining

$$u(x,t) := \begin{cases} u_1(x,t), & x < 0, \\ u_2(x,t), & x > 0. \end{cases}$$

This function satisfies the desired partial differential equation in each domain, but fails to satisfy the continuity condition $u \in C^1(-\infty,\infty)$ at the origin. A straightforward application of potential theory [4] yields the correct solution

$$u(x,t+\tau) := \begin{cases} u_1(x,t+\tau) - \frac{c_1}{c_1+c_2} a(\tau + \frac{x}{c1}) - \frac{c_1 c_2}{c_1+c_2} \int_0^{\tau+\frac{x}{c_1}} b(s)\,\mathrm{d}s & x < 0, \\ u_2(x,t+\tau) + \frac{c_2}{c_1+c_2} a(\tau - \frac{x}{c2}) - \frac{c_1 c_2}{c_1+c_2} \int_0^{\tau-\frac{x}{c_2}} b(s)\,\mathrm{d}s & x > 0, \end{cases} \tag{18}$$

where

$$a(s) := u_1(0,t+s) - u_2(0,t+s), \tag{19}$$

$$b(s) := \frac{\partial}{\partial x} u_1(0,t+s) - \frac{\partial}{\partial x} u_2(0,t+s). \tag{20}$$

In order to obtain a numerical method based on the formula (18), we can use the algorithms described in the preceding sections with a few simple modifications:

1. Use the formulas in (16) and (17)to evolve $u_1$ and $u_2$ separately for a time step at all grid points $x_i$.
2. Compute the correction terms in (18)from $a(s)$ and $b(s)$, which can be derived analytically from $u_1$ and $u_2$.
3. If solving a Dirichlet problem on a finite interval, such as $[-1,1]$, use boundary corrections $\Psi$ as described in Section 2.

## 7. Numerical results

In this section, we provide numerical results concerning the accuracy and stability of a variety of schemes based on the paradigm described above. The stability of a scheme is determined numerically by looking at the spectral radius of its evolution matrix for a variety of grid sizes. The accuracy of a scheme is determined by experiments using several test functions. We assume that the grid is uniform away from the boundary, with uniform spatial discretization $\Delta x$ except for irregular cells near the boundary of size $E$ which may be much smaller than $\Delta x$.

A scheme is denoted by $S^p_{\{m,l\}}(r)$ if it fits function values by a polynomial of order $p$ in each cell using $p+1+m$ nearby grid points. If the domain contains small cells, $p+1+m+l$ points are used to fit the polynomial near the small cells to ensure that the interpolation process is not too ill-conditioned even if the small cells are orders of magnitude smaller than $\Delta x$. If the grid is uniform, then the parameter $l$ is not invoked and the scheme can be denoted by $S^p_m(r)$. The time step and the spatial discretization are related by $\Delta t = r\Delta x$. If there are two wave speeds in the problem domain, we allow the spatial discretization to be different in the two regions. A scheme will be denoted by $S^p_{\{m,l\}}(r_1,r_2)$ where $\Delta x_1 = \Delta t/r_1$ and $\Delta x_2 = \Delta t/r_2$ are the spatial discretizations in the two regions.

As noted earlier, if $p+1+m$ is even, the scheme is said to have a symmetric stencil; otherwise, it has a non-symmetric stencil. If $m = 0$, the scheme is interpolatory; otherwise, it is a least squares fit. It is strongly consistent if it uses (6). It is strongly $u$-consistent if it uses (9).

### 7.1. Periodic boundary conditions

We begin with the simplest case: periodic boundary conditions, which avoids the need for incorporating boundary corrections. The test functions used to obtain convergence results are $\sin(2\pi(x \pm t))$, $\sin(4\pi(x \pm t))$, and $\sin(6\pi(x \pm t))$ on the interval $[0, 1]$. The spatial grid is $\{x_1, x_2, \ldots, x_{M-1}, x_M\}$, where the point $x_1$ is identified with the point $x_{M+1}$. We let the grid be uniform from $x_2$ to $x_{M+1}$ with spacing $\Delta x$. The irregular cell $[x_1, x_2]$ is of length $E$.

A simple calculation shows that, for uniform grids, the stencil generated by the strongly $u$-consistent approach reduces to the exact "symmetric D'Alembert formula":

$$U_i^{n+1} = -U_i^{n-1} + U_{i-1}^n + U_{i+1}^n,$$

for any polynomial approximation order $p \geqslant 2$. The stencil in the strongly consistent approach reduces to

$$U_i^{n+1} = -U_i^{n-1} + U_{i-1}^n + U_{i+1}^n + \Delta t[U_x^{i-1}(x_i, t_n) - U_x^i(x_i, t_n)].$$

Thus, strong consistency deviates from the exact formula by $-\Delta t J^{x_i}_{U_x(x,t_n)}$.

Table 1 shows the numerical convergence of the strongly consistent and strongly $u$-consistent schemes $S_0^p(1)$ for $p = 2, \ldots, 9$ on a uniform grid using the sine test functions by the usual von Neumann analysis. Unstable schemes are denoted by 'd'. Fig. 3 shows that for $S_0^8(1)$ the incorporation of the discontinuities of $U(x, t_n)$ and $U(x, t_{n-1})$ into the evolution formula moves originally unstable eigenvalues onto the unit circle.

Table 2 shows the numerical convergence of the schemes $S_m^p(r)$, $r = \Delta t/\Delta x = \{0.9, 1.1\}$, $m = \{0, 1, 2\}$, $p = \{2, \ldots, 9\}$ on a uniform grid. Without enforcing strong $u$-consistency, interpolatory schemes ($m = 0$) with symmetric stencils are stable, as are $S_1^2(0.9)$ and $S_1^2(1.1)$. All others are unstable. By enforcing strong $u$-consistency, all schemes with symmetric stencils are stable and converge at the expected orders. Fig. 4 illustrates how the eigenvalues of the schemes $S_1^8(1.1)$ and $S_2^9(1.1)$ are pushed into the unit circle by enforcing strong $u$-consistency. They are no longer on the unit circle because the discrete evolution scheme is no longer time-symmetric.

Table 3 shows the numerical convergence of the strongly $u$-consistent schemes $S^p_{\{m,l\}}(r)$, $r = \{0.9, 1.0, 1.1\}$, $m = \{0, \ldots, 3\}$, $l = \{0, 1\}$, $p = \{2, \ldots, 9\}$ on a grid with an irregular cell. The irregular cell sizes tested are $E = \{\Delta x, 0.1\Delta x, 10^{-6}\Delta x\}$. The schemes marked as convergent are stable for all three irregular cell sizes, while the schemes marked as unstable are unstable for at least one cell size. The scheme $S^3_{\{3,0\}}(0.9)$ is not stable, whereas $S^3_{\{3,0\}}(1.1)$ is second-order accurate. In all other entries, there is no difference between the behavior of $r = 0.9$ and $r = 1.1$. Overall, one can see again that symmetric stencils are favored.

Table 1
Numerical convergence of interpolatory schemes $S_0^p(1)$ on the interval $[0, 1]$ with periodic boundary conditions on a uniform grid of size $M = \{20, 40, 80, 100\}$

| Convergence orders of schemes $S_0^p(1)$ | | | | | | | | |
|---|---|---|---|---|---|---|---|---|
| $p$ | 2 | 3 | 4 | 5 | 6 | 7 | 8 | 9 |
| Strongly consistent | d | 2 | d | 4 | d | 6 | d | 8 |
| Strongly $u$-consistent | exa | exa | exa | exa | exa | exa | exa | exa |

The exact solutions tested are $\sin(2\pi(x \pm t))$, $\sin(4\pi(x \pm t))$, and $\sin(6\pi(x \pm t))$. The scheme $S_m^p(r)$ uses the time step $\Delta t = r\Delta x$ and a piecewise polynomial approximation of degree $p$ based on the nearest $p + 1 + m$ points. The table shows the convergence orders of various schemes: 'd' denotes that the scheme is unstable, 'exa' denotes that the approximation is exact. The strongly $u$-consistent schemes are exact for this model problem.

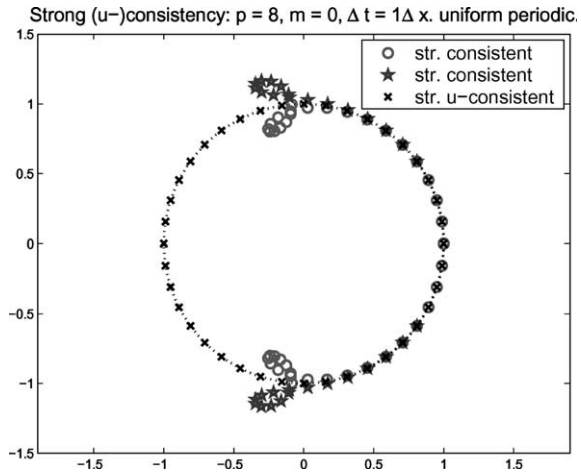


Fig. 3. Eigenvalues of the evolution matrix of the $S_0^8(1)$ schemes for the uniform periodic case. The circles and the stars denote the stable and unstable eigenvalues of the strongly consistent scheme, respectively. The "×"s denote the eigenvalues of the strongly $u$-consistent scheme, all of which are stable. The unit circle is outlined in dots.

Table 2
Numerical convergence of schemes $S_m^p(r)$, $r = \{0.9, 1.1\}$, $m = \{0, 1, 2\}$ on the interval $[0, 1]$ subject to periodic boundary conditions on a uniform grid of size $M = \{20, 40, 80, 100\}$

| Convergence orders of schemes $S_m^p(r)$ | | | | | | | | |
|---|---|---|---|---|---|---|---|---|
| $p$ | 2 | 3 | 4 | 5 | 6 | 7 | 8 | 9 |
| $S_0^p(0.9)$ and $S_0^p(1.1)$ | | | | | | | | |
| Strongly consistent | d | 2 | d | 4 | d | 6 | d | 8 |
| Strongly $u$-consistent | d | 2 | d | 4 | d | 6 | d | 8 |
| $S_1^p(0.9)$ and $S_1^p(1.1)$ | | | | | | | | |
| Strongly consistent | 2 | d | d | d | d | d | d | d |
| Strongly $u$-consistent | 2 | d | 4 | d | 6 | d | 8 | d |
| $S_2^p(0.9)$ and $S_2^p(1.1)$ | | | | | | | | |
| Strongly consistent | d | d | d | d | d | d | d | d |
| Strongly $u$-consistent | d | 2 | d | 4 | d | 6 | d | 8 |

The exact solutions tested are $\sin(2\pi(x \pm t))$, $\sin(4\pi(x \pm t))$, and $\sin(6\pi(x \pm t))$. The scheme $S_m^p(r)$ uses the time step $\Delta t = r\Delta x$ and a piecewise polynomial approximation to the solution of degree $p$, using the nearest $p + 1 + m$ data points. With the exceptions of $S_1^2(0.9)$ and $S_1^2(1.1)$, the non-interpolatory ($m \neq 0$) strongly consistent schemes are unstable. Enforcing strong $u$-consistency stabilized those schemes with symmetric stencils, i.e., those with $p + 1 + m$ even.

### 7.2. Dirichlet boundary conditions

For the wave equation on $[a, b]$ subject to Dirichlet boundary conditions, the evolution formula with boundary correction has been implemented. The test functions used to obtain numerical convergence results are left and right moving sine waves, polynomials, and exponentials on the interval $[0, 1]$. The spatial grid is $\{a = x_1, x_2, \ldots, x_{M-1}, x_M = b\}$. The size of the two irregular cells near the boundary is $E = x_2 - x_1 = x_M - x_{M-1}$, and the size of the uniform cells is $\Delta x = x_i - x_{i-1},\ i = 3, \ldots, M - 1$.

We have carried out standard matrix stability analysis for homogeneous boundary conditions numerically for a variety of grid sizes, and verified the convergence of strongly $u$-consistent schemes up to order 9

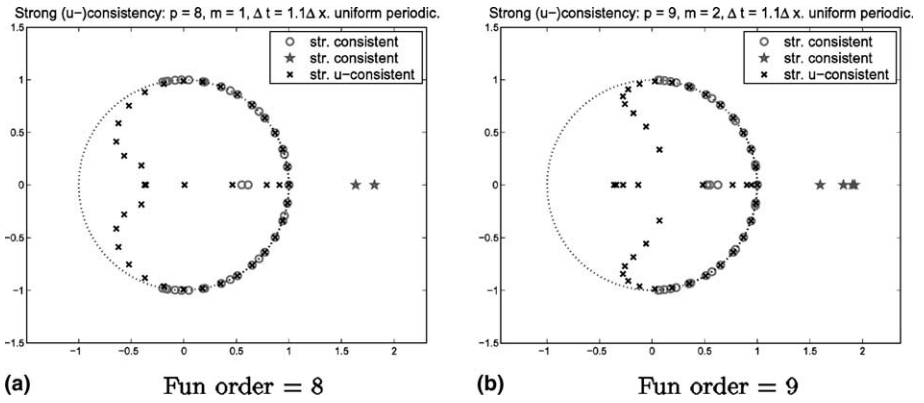


Fig. 4. Eigenvalues of the evolution matrix of the non-interpolatory $S_1^8(1.1)$ and $S_2^9(1.1)$ schemes for the uniform periodic case. The circles and the stars denote the stable and unstable eigenvalues of the strongly consistent scheme, respectively. The "×"s denote the eigenvalues of the strongly $u$-consistent scheme, all of which are stable. The unit circle is outlined in dots.

Table 3
Numerical convergence of strongly $u$-consistent schemes $S^p_{\{m,l\}}(r)$, $m = \{0,1,2,3\}$, $r = \{0.9, 1.0, 1.1\}$ for the wave equation on the interval $[0,1]$ subject to periodic boundary conditions on a grid of size $M = \{20, 40, 80, 100\}$ with an irregular cell of size $E = \{1.0\Delta x, 0.1\Delta x, 10^{-6}\Delta x\}$

| Convergence of strongly $u$-consistent schemes $S^p_{\{m,l\}}(r)$ | | | | | | | | |
|---|---|---|---|---|---|---|---|---|
| $p$ | 2 | 3 | 4 | 5 | 6 | 7 | 8 | 9 |
| $S^p_{\{0,1\}}$ | | | | | | | | |
| $\Delta t = 1.0\Delta x$ | 3 | 3 | 5 | 5 | 7 | 7 | 9 | 9 |
| $\Delta t = \{0.9, 1.1\}\Delta x$ | d | 2 | d | d | d | d | d | d |
| $S^p_{\{1,1\}}$ | | | | | | | | |
| $\Delta t = 1.0\Delta x$ | 2 | d | 4 | d | 6 | d | 8 | 8 |
| $\Delta t = \{0.9, 1.1\}\Delta x$ | 2 | d | 4 | d | 6 | d | 8 | d |
| $S^p_{\{2,0\}}$ | | | | | | | | |
| $\Delta t = 1.0\Delta x$ | d | 2 | d | 4 | d | 6 | d | d |
| $\Delta t = \{0.9, 1.1\}\Delta x$ | d | 2 | d | 4 | d | 6 | d | 8 |
| $S^p_{\{3,0\}}$ | | | | | | | | |
| $\Delta t = 1.0\Delta x$ | 2 | 2 | 4 | 4 | 6 | 6 | 8 | 8 |
| $\Delta t = \{0.9, 1.1\}\Delta x$ | 2 | d,2(*) | 4 | d | 6 | d | 8 | d |

The exact solutions tested are $\sin(2\pi(x \pm t))$, $\sin(4\pi(x \pm t))$, and $\sin(6\pi(x \pm t))$. The scheme $S^p_{\{m,l\}}(r)$ is the same as $S^p_m(r)$ except $l$ extra points are added to solve the local approximation/interpolation problem near the small cell. A scheme is called stable (denoted by a convergence order) if it is stable for all three irregular cell sizes. A scheme is called unstable (denoted by 'd') if it is unstable for any of the three irregular cell sizes. The entry marked by * in the last row of the table is meant to indicate that $S^3_{\{3,0\}}(0.9)$ is unstable whereas $S^3_{\{3,0\}}(1.1)$ is second-order accurate.

in the presence of irregular cells of size $E = \{\Delta x, 0.1\Delta x, 10^{-6}\Delta x\}$. The results are summarized in Table 4. The schemes $S^6_{\{1,l\}}(1.1)$, $S^8_{\{2,l\}}(1.1)$, and $S^9_{\{3,l\}}(1.1)$ are stable only when $l = 1$. The numerical domain of dependence grows as one goes down the table, and it is perhaps not surprising that more schemes become stable. The eigenvalues of the strongly consistent and the strongly $u$-consistent $S^4_1(1)$ schemes are shown in Fig. 5.

Table 4
Numerical convergence of the strongly $u$-consistent schemes $S^p_{\{m,l\}}(r)$, $m = \{0,1,2,3\}$, $r = \{0.9, 1.0, 1.1\}$, and $l = \{0,1\}$ while solving $u_{tt} = u_{xx}$ on the interval $[0,1]$ subject to Dirichlet boundary conditions on a grid of size $M = \{20, 40, 80, 100\}$

| Convergence orders of strongly $u$-consistent schemes $S^p_{\{m,l\}}(r)$ | | | | | | | | |
|---|---|---|---|---|---|---|---|---|
| $p$ | 2 | 3 | 4 | 5 | 6 | 7 | 8 | 9 |
| $S^p_{\{0,1\}}$ | | | | | | | | |
| $\Delta t = 1.0\Delta x$ | d | 5 | 5 | 7 | d | d | d | d |
| $\Delta t = 0.9\Delta x$ | 1 | 3 | 3 | 5 | d | d | d | d |
| $\Delta t = 1.1\Delta x$ | d | 3 | d | d | d | d | d | d |
| $S^p_{\{1,0\}}$ and $S^p_{\{1,1\}}$ | | | | | | | | |
| $\Delta t = 1.0\Delta x$ | 3 | 3 | 5 | 5 | d | d | d | d |
| $\Delta t = 0.9\Delta x$ | 3 | d | 5 | d | 7 | d | d | d |
| $\Delta t = 1.1\Delta x$ | 3 | 3 | 5 | 5 | 6* | d | d | d |
| $S^p_{\{2,0\}}$ and $S^p_{\{2,1\}}$ | | | | | | | | |
| $\Delta t = 1.0\Delta x$ | 1 | 3 | 3 | 5 | 5 | d | d | d |
| $\Delta t = 0.9\Delta x$ | 1 | 3 | 3 | 5 | d | d | d | d |
| $\Delta t = 1.1\Delta x$ | 1 | 3 | 3 | 5 | 5 | 7 | 7* | d |
| $S^p_{\{3,0\}}$ and $S^p_{\{3,1\}}$ | | | | | | | | |
| $\Delta t = 1.0\Delta x$ | 3 | 3 | 5 | 5 | 7 | 7 | d | d |
| $\Delta t = 0.9\Delta x$ | 3 | 3 | 5 | 5 | 7 | d | d | d |
| $\Delta t = 1.1\Delta x$ | 4 | 4 | 5 | 5 | 6 | 7 | 8 | 9* |

Two irregular cells were introduced near the boundary points of length $E = \{1.0\Delta x, 0.1\Delta x, 10^{-6}\Delta x\}$. The exact solutions tested are left and right moving sine waves, polynomials, and exponentials. A scheme is called stable (denoted by a convergence order) if it is stable for all three irregular cell sizes. A scheme is called unstable (denoted by 'd') if it is unstable for any of the three irregular cell sizes. Some entries are marked by a *; for these, only the schemes with $l = 1$ are stable, the schemes with $l = 0$ are unstable.

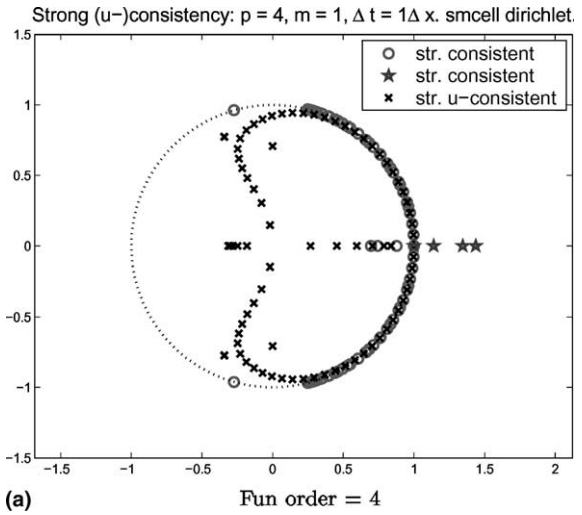


Fig. 5. Eigenvalues of the evolution matrix of the $S^4_1(1.0)$ schemes on a grid with two small cells near the boundary of size $10^{-6}\Delta x$ subject to Dirichlet boundary conditions. The circles and the stars denote the stable and unstable eigenvalues of the strongly consistent scheme, respectively. The "×"s denote the eigenvalues of the strongly $u$-consistent scheme, all of which are stable. The unit circle is outlined in dots.

### 7.3. Multiple wave speeds

We solve $u_{tt} = u_{xx}$, $x < 0$, $u_{tt} = (0.5)^2 u_{xx}$, $x > 0$ on the interval $[-1, 1]$ with Dirichlet boundary conditions and show numerical results. In Tables 5 and 6 the exact solution tested is obtained by letting $u_1(x,t) = -1.8\cos(3\pi(x-t))$ and $u_2(x,t) = 0.2\sin(2\pi(x+0.5t))$ according to (18). The grid has uniform spacing away from the boundary, $\Delta x_1 = \Delta t/r_1$ to the left of the interface and $\Delta x_2 = \Delta t/r_2$ to the right of the interface. Two irregular cells were introduced near the boundaries of length $E = \{1.0\Delta x, 0.1\Delta x, 10^{-6}\Delta x\}$. Stability is determined numerically by looking at the spectral radius of the evolution matrix.

In Table 5, $\Delta x_1 = \Delta t, \Delta x_2 = \Delta t$ and fourth order accurate schemes can be obtained in the strongly $u$-consistent case.

Table 5
Numerical convergence of schemes $S^p_{\{m,l\}}(r_1, r_2)$ while solving $u_{tt} = u_{xx}$, $x < 0$, $u_{tt} = (0.5)^2 u_{xx}$, $x > 0$ on the interval $[-1, 1]$ subject to Dirichlet boundary conditions on a grid of size $M = \{30, 60, 120, 200\}$ with two irregular cells near the boundary of size $E = \{\Delta x, 0.1\Delta x, 10^{-6}\Delta x\}$

| Convergence orders of schemes $S^p_m(r)$ | | | | | | | |
|---|---|---|---|---|---|---|---|
| $p$ | 2 | 3 | 4 | 5 | 6 | 7 | 8 |
| $S^p_{\{0,1\}}(1,1)$ | | | | | | | |
| Strongly consistent | d | 2 | d | d | d | d | d |
| Strongly $u$-consistent | d | 2 | 3 | 4 | d | d | d |
| $S^p_{\{1,0\}}(1,1)$ | | | | | | | |
| Strongly consistent | d | d | d | d | d | d | d |
| Strongly $u$-consistent | 2 | 2 | 4 | 4 | d | d | d |
| $S^p_{\{2,0\}}(1,1)$ | | | | | | | |
| Strongly consistent | d | d | d | d | d | d | d |
| Strongly $u$-consistent | s | 2 | 3 | 4 | d | d | d |

Here, $\Delta x_1 = \Delta x_2 = \Delta t$. A scheme is called stable (denoted by a convergence order) if it is stable for all three irregular cell sizes. A scheme is called unstable (denoted by 'd') if it is unstable for any of the three irregular cell sizes.

Table 6
Numerical convergence of schemes $S^p_{\{m,l\}}(r_1, r_2)$ while solving $u_{tt} = u_{xx}$, $x < 0$, $u_{tt} = (0.5)^2 u_{xx}$, $x > 0$ on the interval $[-1, 1]$ subject to Dirichlet boundary conditions on a grid of size $M = \{30, 60, 120, 200\}$ with two irregular cells near the boundary of size $E = \{\Delta x, 0.1\Delta x, 10^{-6}\Delta x\}$

| Convergence orders of schemes $S^p_m(r)$ | | | | | | | |
|---|---|---|---|---|---|---|---|
| $p$ | 2 | 3 | 4 | 5 | 6 | 7 | 8 |
| $S^p_{\{0,1\}}(1,2)$ | | | | | | | |
| Strongly consistent | d | 2 | d | d | d | d | d |
| Strongly $u$-consistent | d | 4 | 5 | 6 | d | d | d |
| $S^p_{\{1,0\}}(1,2)$ | | | | | | | |
| Strongly consistent | d | d | d | d | d | d | d |
| Strongly $u$-consistent | 2 | 2 | 4 | 4 | d | d | d |
| $S^p_{\{2,0\}}(1,2)$ | | | | | | | |
| Strongly consistent | d | d | d | d | d | d | d |
| Strongly $u$-consistent | 1 | 2 | 3 | 4 | 5 | d | d |

Here, $\Delta x_1 = \Delta t$ and $\Delta x_2 = 0.5\Delta t$. A scheme is called stable (denoted by a convergence order) if it is stable for all three irregular cell sizes. A scheme is called unstable (denoted by 'd') if it is unstable for any of the three irregular cell sizes.

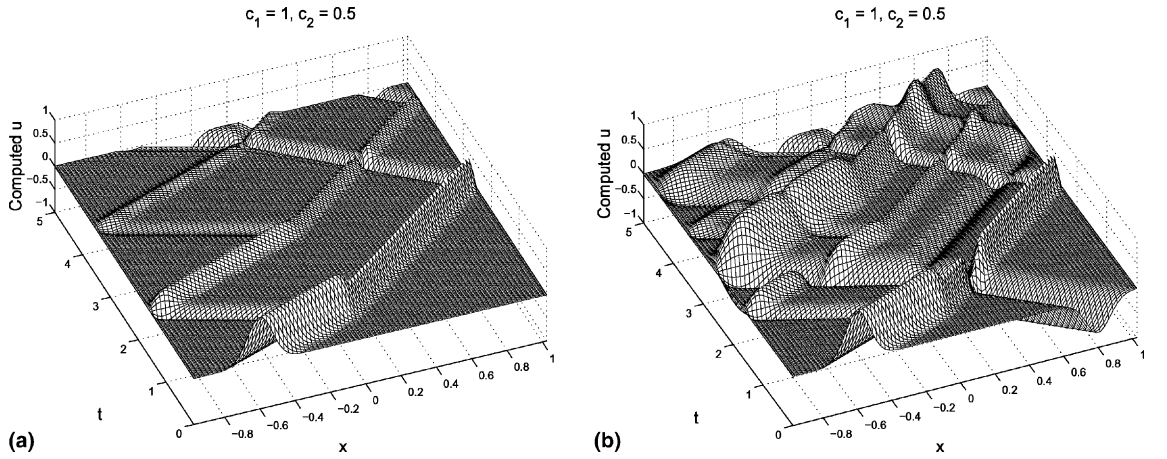


Fig. 6. Solution of $u_{tt} = u_{xx}$, $x < 0$, $u_{tt} = (0.5)^2 u_{xx}$, $x > 0$ on the interval $[-1, 1]$ subject to homogeneous Dirichlet boundary conditions, $u(-1, t) = 0, u(1, t) = 0$, on a grid of size 160 with two small cells near the boundary of size $10^{-6}\Delta x$. The numerical scheme is the strongly $u$-consistent $S^5_{\{0,1\}}(1, 1)$, which is fourth-order accurate. The spatial discretization is $\Delta x_1 = \Delta t$ to the left of $x = 0$ and $\Delta x_2 = \Delta t$ to the right of $x = 0$. The initial data consist of Gaussians. Note waves being reflected and transmitted at the interface. (a) One initially right miving Gaussian. (b) One initially right and one initially left moving Gaussian.

In Table 6, $\Delta x_1 = \Delta t, \Delta x_2 = 0.5\Delta t$ and sixth-order accurate schemes are available in the strongly $u$-consistent case.

In Fig. 6(a) we let $u_1(x, t) = 1.0\mathrm{e}^{-(10(x-t+0.6))^2}$, a right moving Gaussian initially centered at $-0.6$, and let $u_2(x, t) = 0$ according to (18). In Fig. 6(b) we let $u_1(x, t) = 1.0\mathrm{e}^{-(10(x-t+0.6))^2}$ and let $u_2(x, t) = -0.7\mathrm{e}^{-(10(x+0.5t-0.8))^2}$, a left moving Gaussian initially centered at 0.8. We imposed homogeneous Dirichlet boundary conditions, $u(-1, t) = 0, u(1, t) = 0$, which are satisfied by the initial data with an exponentially small error. The scheme we used is the strongly $u$-consistent $S^5_{\{0,1\}}(1, 1)$, which is fourth-order accurate. The grid size is 160 and there are two cells near of the boundary of size $10^{-6}\Delta x$. In both figures, one can see waves being reflected and transmitted at the interface.

## 8. Conclusions

We have implemented an integral evolution formula for the wave equation and introduced the notion of strongly $u$-consistent evolution schemes. A strongly $u$-consistent scheme is one which treats the approximation to the solution as a single-valued function at each time step. The schemes obtained in this way have high order accuracy and many appear to be stable and robust in the presence of small cells, allowing time steps to be determined according to the uniform spatial grid spacing. We conjecture that a direct proof of convergence is possible.

The work involved in strongly $u$-consistent schemes is essentially the same as that for any other explicit marching scheme. The cost per time step is $\mathrm{O}(MK)$, where $K$ is the number of grid points in the numerical domain of dependence and $M$ is the number of grid points.

Higher dimensional analysis will be reported at a later date. Preliminary experiments with fourth-order accurate stencils on a square domain with irregular meshes appear promising, but are technically more involved. Strong $u$-consistency, for example, involves Dirac $\delta$-functions distributed on line segments which form the boundaries of two-dimensional cells.

## References

[1] B. Alpert, L. Greengard, T. Hagstrom, An integral evolution formula for the wave equation, J. Comput. Phys. 162 (2) (2000) 536–543.
[2] M.J. Berger, R.J. LeVeque, A rotated difference scheme for cartesian grids in complex geometries, in: Proceedings, AIAA 10th Computational Fluid Dynamics Conference, Honolulu, Hawaii, 1991, pp. 1–9 (AIAA Paper CP-91-1602).
[3] W.J. Coirier, K.G. Powell, An accuracy assessment of Cartesian-mesh approaches for the Euler equations, J. Comput. Phys. 117 (1) (1995) 121–131.
[4] R.B. Guenther, J.W. Lee, Partial Differential Equations of Mathematical Physics and Integral Equations, Prentice-Hall, Englewood Cliffs, NJ, 1988.
[5] R.J. LeVeque, A large time step generalization of Godunov's method for systems of conservation laws, SIAM J. Numer. Anal. 22 (6) (1985) 1051–1073.
[6] J.J. Quirk, An alternative to unstructured grids for computing gas dynamic flows around arbitrarily complex two-dimensional bodies, Comput. Fluids 23 (1) (1994) 125–142.
[7] R.D. Richtmyer, K.W. Morton, Difference Methods for Initial-Value Problems, Interscience Publishers/Wiley, New York–London–Sydney, 1967.
[8] J.C. Strikwerda, Finite Difference Schemes and Partial Differential Equations, Wadsworth & Brooks/Cole Advanced Books & Software, Pacific Grove, CA, 1989.